Original Article

Modeling and optimization of A-GTAW process using Box–Behnken design and hybrid BPNN-PSO approach

Masoud Azadi Moghaddam and Farhad Kolahan

Abstract

Gas tungsten arc welding (GTAW) is the most extensively used process capable of fabricating a wide range of alloys based on its distinctive merits has been introduced. However, some demerits have been reported among which shallow penetration is the most crucial ones. In order to deal with the poor penetration of the process, different procedures have been proposed among which activated gas tungsten arc welding (A-GTAW) is the most extensively used one. In this study effect of percentage of activating fluxes (TiO_2 and SiO_2) combination (F) and the most important process variables (welding current (C), welding speed (S)) on the most important process measures (weld bead width (WBW), depth of penetration (DOP), and consequently aspect ratio (ASR)) in welding of AISI316L austenite stainless steel parts have been investigated. Box-behnken design (BBD) has been used to design the experimental matrix required for date gathering, modeling, and statistical analysis purposes. A neural network with a back propagation algorithm (BPNN) in artificial neural network (ANN) modeling approach has been employed to relate the process input variables and output characteristics. The proper BPNN architecture (number of hidden layers and neurons/nodes in each hidden layer) has been determined using particle swarm optimization (PSO) algorithm. Moreover, process optimization in such a way that maximum DOP, minimum WBW, and desired ASR achieved has been carried out using PSO algorithm. Next, the performance of PSO algorithm has been checked using simulated annealing (SA) algorithm. Finally, to evaluate the performance of the proposed method a set of confirmation experimental test has been conducted. Results of experimental tests revealed that the proposed method is quite efficient in modeling and optimization (with less than 4% error) of A-GTAW process.

Introduction

Tungsten inert gas (TIG) welding known as gas tungsten arc welding (GTAW) process due to its high level of process control and is the most useful fabrication process used for a wide range of alloys among which stainless steels are the most important ones. However, shallow depth of penetration (DOP) in this process required multi-pass welding for thick (more than 3 mm) weldments. In this regard, different procedures have been proposed to enhance the process among which using activating fluxes known as activated gas tungsten arc welding (A-GTAW) process is the most extensively used ones.[1–5] Before the GTAW process has been started, a layer of activating flux or fluxes (including oxides, fluorides, and chlorides) on the surface of weldment is coated. As the welding process proceeds due to the activating flux melting and consequently incorporating into the weld pool arc constriction and reversal of

Marangoni convection phenomena occurred.[4] Therefore, the surface tension gradient direction changed from a negative value $((\partial\sigma/\partial\ T) < 0)$ to a positive value $((\partial\sigma/\partial\ T) > 0)$, and consequently the molten metal movement changed from the welding boundary towards the center of the weld pool (inward movement). Hence, based on the reversal of Marangoni convection and arc constriction phenomena, DOP increased and consequently weld bead width (WBW) and heat affected zone (HAZ) area decreased.[5] Smaller WBW and HAZ values lead to higher corrosion resistance.[6]

[1]Department of Mechanical Engineering, Ferdowsi University of Mashhad, Mashhad, Iran

Corresponding author:
Farhad Kolahan, Department of Mechanical Engineering, Ferdowsi University of Mashhad, Mashhad, Iran.
Email: kolahan@um.ac.ir

Several phases have been reported for Ferritic steels (Ferrite, Pearlite and Martensite) all of which have body-centered cubic (one atom at the eight corners of a cube and one in the center of the cube) crystal structure. The primary phase of austenitic steels is austenite with face-centered cubic (one atom at the eight corners of a cube and one in the center of each of the six faces) crystal structure. The unit cell of BCC has one sphere in the center of the cube and eight spheres at the corners. Then, the total number of spheres present in a BCC unit cell is 9.[6] The unit cell of the FCC has eight spheres at each corner and one sphere at the center of each cubic face. Then the unit cell of FCC has 12 spheres. The packing factor of FCC and BCC structures are 0.74 and 0.68 respectively. As the slip phenomenon in the crystal structure with a greater planer density in the chosen direction will progress with more ease. Thus, metals with FCC crystal structure deform easier than BCC ones and are more ductile. Therefore, BCC structures are stronger than FCC structures.[6] Austenite and delta-ferrite have FCC and BCC crystal structures respectively. The delta-ferrite content in the weld metals is increased using A-GTAW process. Thus, a beneficial effect in increasing the strength of AISI316L weldments is made using A-GTAW process of austenite stainless steel parts.[6]

Based on the literature review A-GTAW process is capable of fabricating different materials namely: titanium, aluminum, manganese, and stainless steel (including austenite and austenite duplex) alloys.[1–10] For fabricating of weldments thickness of which exceeds 3 mm using GTAW process, a gap between the welding parts is considered filling of which required using filler metal. Whereas, elimination of edge preparation and welding in a single pass for fabricating weldments with 8 mm thickness without even using filler metal has been reported using A-GTAW process.[7] There is a great deal of studies in which different aspects of A- GTAW welding process has been taken into account.[1–14] In this regard, an attempt has been done to investigate the effect of using activating flux and filler metal wire in A-TIG and TIG welding process of Inconel 625 respectively. In this regard, mechanical properties and microstructural characteristics have been studied. Based on the tensile tests, failures have been observed at the weld zone in both welding processes. Furthermore, Charpy impact test revealed that A-TIG welded specimens had low toughness value compared to the TIG welded weldments. An outstanding corrosion resistance has been reported for A-GTAW process.[1]

Effect of flux and flux gap on the mechanical properties and weld bead geometry (WBG) of flux bounded tungsten inert gas (FBTIG) welding process of Inconel 600 alloy (bead-on-plate welding and butt weld joints) has been studied. Based on the obtained results, DOP has been increased three times for FBTIG welding process using SiO_2 flux and 2.5 mm flux gap. Moreover, tensile strength at the room temperature for FBTIG welded specimens has been increased. Furthermore, it has been concluded that multi-pass TIG welding process could be replaced by single-pass FBTIG welding process in order to join thick weldments (with more than 3 mm thickness) of Inconel 600 alloy.[2]

In order to recognize the effect of adding an activating flux on aspect ratio of weld geometry and hardness (Brinell) of Inconel 625 alloy in A-GTAW process, Taguchi method (L_{25} orthogonal array) has been used. Welding current, torch travel speed, and arc gap have been considered as the process input variables. Experimental results revealed that torch travel speed at 75 mm/min, welding current at 300 Amps, and arc gap of 1 mm results in optimum condition with 262 Brinell hardness and aspect ratio of 0.421.[3]

The effect of SiO_2, MnO_2, TiO_2, and Al_2O_3 activating fluxes on elongation, yield strength (YS), and ultimate tensile strength (UTS) of duplex stainless steel SS2205 has been investigated. The experimental test results revealed that using SiO_2, MnO_2, TiO_2, and Al_2O_3 activating fluxes leads to an improvement in TIG welding process by increasing DOP, and reducing the angular distortion.[4]

In a research microstructural and mechanical properties of weldments fabricated using A-GTAW process has been studied. Based on the achieved results, using activating fluxes enhances the welding process performance.[6] Response surface methodology (RSM) has been employed to model and optimize the A-GTAW process in order to achieve the largest DOP by Pamnani et al.[7] GTAW process with and without activating fluxes have been studied by Kumar et al.[12] Based on the results, full penetration has been reported for A-GTAW process. Furthermore, using activating fluxes could improve the performance of GTAW process by increasing DOP and decreasing WBW simultaneously. Venkatesan et al.[13] reported by using activating fluxes edge preparation before welding process (for specimens with more than 3 mm thickness) could be eliminated. Moreover, welding passes required for accomplishing fabricating process has been decreased using activating fluxes. An improvement in mechanical properties and distortion reduction have been reported as the main assets of A-GTAW process by Chern et al.[14] Effect of using oxide, chloride, and fluoride fluxes in dissimilar welding process of stainless steel and low alloy parts have been investigated by Tathgir et al.[15] The largest DOP has been reported for oxide-based fluxes. Moreover, other fluxes had trivial and negligible effect on DOP.

Based on the process literature review, there is a great deal of studies in which different aspects of A-GTAW process have been investigated.[1–14] In these studies, the effect of adding activating fluxes has been investigated. However, the lack of modeling, statistical analysis in order to determine the percent contribution of each process input variables on the process outputs, and multi-criteria optimization of the process senses. To the best of our knowledge, there is no study in which modeling, statistical analysis, and multi-criteria optimization (achieving maximum DOP, minimum WBW and required value for ASR simultaneously) of A-GTAW process output characteristics have been considered

using design of experiments (DOE) approach for designing experimental matrix, back propagation neural network (BPNN) method for modeling of the process, and SA and PSO algorithms for optimization purposes. In this study effect of the process input variables including welding speed and welding current has been investigated. Moreover, percentage combination of the two most extensively used activating fluxes (TiO_2 and SiO_2) has been considered as an adjusting variable in order to be optimized in such a way that the maximum DOP, minimum WBW and the proper value for ASR achieved simultaneously. Therefore, percentage of activating fluxes combination (F), welding current (I), and welding speed (S) have been considered as the process input variables selecting of which has been done based on the literature survey review, and some preliminary experimental (screening approach) have been conducted. In order to determine the interval and levels of each process variables, screening approach has been conducted. Based on the number of process input variables and their corresponding levels, different design of experiments could be proposed among which the most appropriate one is box-behnken design considered in this study. Next, in order to establish the relationships between process input and output parameters, BPNN has been employed. Next, PSO algorithm has been used in order to determine the best BPNN architecture (number of hidden layers and number of nodes/neurons in each layer). Finally, to determine the best values for process input variables for multi-criteria optimization of the process, PSO algorithm has been used. Moreover, the adequacy of the PSO algorithm has been checked using SA algorithm in order to avoid getting trapped in local minima. The proposed method for modeling and optimization has been conducted on AISI316L austenitic stainless steel specimens. Based on the achieved results, an optimum process input variables values and optimized activating fluxes formula ($TiO_2 + SiO_2$) have been proposed in such a way that maximum DOP with minimum WBW and desired ASR achieved simultaneously.

Empirical set up and equipment used

Determination of process variables and their corresponding intervals and levels

In order to determine the crucial process input variables and their corresponding intervals and feasible levels, literature reviews have been studied and some preliminary experimental tests based on the screening method have been conducted. Welding current (I) and welding speed (S) have been determined as the most important variables affecting the A-GTAW process considered in this study.[1–3] Moreover, in order to achieve the merit of percentage of activating fluxes combination (F) effect on the process output characteristics, this parameter has also been considered as a process input variable. To evaluate the A-GTAW process performance, quality characteristics including DOP, WBW, and ASR have been considered to be measured and optimized simultaneously.

In this study some preliminary experimental tests have been conducted and welding references have been studied in order to determine the feasible working intervals of each process input variables and their corresponding levels.[8–14] Based on the screening test findings the process input variables and their corresponding optimum intervals and levels has been determined (Table 1). Other process input variables with negligible effects on the process outputs have been considered at an optimum pre-determined fixed level.

Box-Behnken design (BBD)

In order to arrange an experimental design matrix required for conducting the experiments and gathering the data for modeling and optimization, design of experiments (DOE) approach is used.

Consequently, when the influential process input variables and their corresponding intervals and levels are considered, determination of an appropriate design matrix is the next crucial step. Generally, to establish the relations between process input-output parameters, determine percent contribution of the process influential variables on the output characteristics, and define the optimal levels of input variables in order to get the desired responses, DOE approach is employed.

Recently, one of the most powerful and extensively used method which is used for data gathering, modeling, and statistical analysis purposes is response surface methodology (RSM). RSM includes different approaches among them central composite design (CCD), box–behnken design (BBD) and hybrid family of them are the most important ones.[15–18] In this research, based on the process input variables numbers and their corresponding levels a BBD's L_{17} matrix has been chosen (Table 1).

Material and equipment used

AISI316L stainless steel is an austenitic stainless steel ally and a lower carbon variant of AISI316, both of which contain molybdenum, but the value for AISI316L is more than AISI316. The maximum carbon content of AISI316L is 0.03 which made this alloy to be used where maximum corrosion resistance is required and when post-welding annealing is not possible. Because, AISI316L alloy features better carbide precipitation resistance than AISI316, could be continuously exposed to the temperature of 427°C–857°C (800°F–1575°F), where AISI316 is not advisable to. Food industry; exterior construction in coastal areas; pipeline equipment for the use of marine, chemicals, fertilizer, etc. are the main applications of AISI316L alloy fabricating of which required GTAW process.[19]

In this study, AISI316L austenite stainless steel plates (100 mm × 50 mm × 5 mm) have been considered as specimens on which the experimental tests have been conducted. A paste-like coating which act as activating flux to enhance the process, was made from a combination of Nano oxide fluxes (TiO_2, SiO_2) (+ 99%, 20–30 nm,

Table 1. Experimental BBD matrix and their corresponding measured characteristics.

No.	Flux combination (SiO_2-TiO_2)	Welding speed (mm/sec)	Welding current (I)	Depth of penetration (mm)	Weld bead width (mm)	Aspect ratio (ASR)
1	100	50	175	3.96	6.21	1.57
2	110	50	150	4.65	7.66	1.65
3	110	50	150	5.10	7.58	1.48
4	120	50	125	6.16	6.12	0.99
5	100	50	125	4.84	5.07	1.05
6	110	75	125	5.65	5.74	1.02
7	110	50	150	4.79	8.26	1.72
8	120	75	150	4.95	7.62	1.54
9	120	50	175	4.42	7.64	1.73
10	110	50	150	4.83	7.91	1.64
11	110	25	125	4.58	6.75	1.47
12	110	75	175	3.64	7.82	2.15
13	110	25	175	3.04	7.44	2.44
14	100	75	150	4.03	6.61	1.64
15	110	50	150	4.68	7.96	1.70
16	120	25	150	3.63	7.57	2.08
17	100	25	150	3.15	7.33	2.32

amorphous). FESEM test has been employed in order to determine the powder particle size. The paste-like coating of activating fluxes has been prepared before the welding process begins using mechanical and magnetic mixers for 20 grams of flux mixed with 20 ml of a carrier solvent (methanol).[1,2] Then, the prepared paste-like flux has been applied on the surface of the weldments before the welding process begins using a brush. After evaporation of the carrier solvent, the flux layer remained attached to the surface of the weldment and the welding process could be started.

To carry out the experimental tests based on the L_{17} BBD matrix provided (Table 1), a DIGITIG 250 AC/DC welding machine has been employed. Moreover, Argon (with 99.7% purity) has been used as the shielding inert gas.

Conducting the experimental tests and measuring the results

The experiments have been conducted based on a random order to increase the accuracy of the experiments. DOP,
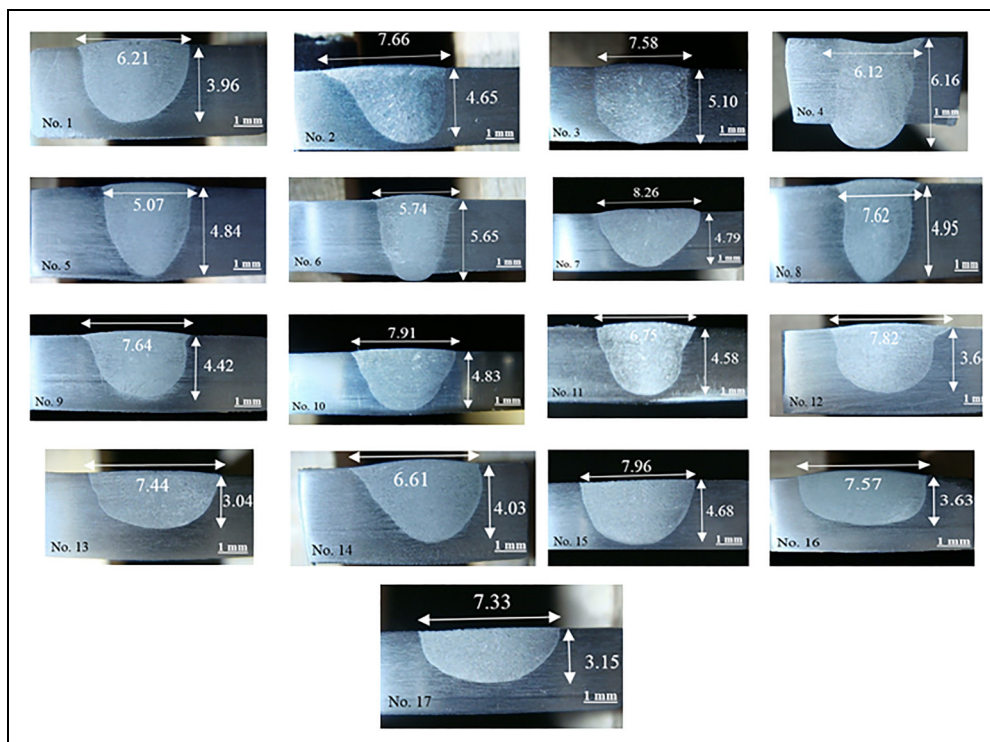

Figure 1. A-GTAW weld cross-sectional profile.

Table 2. Results of analysis of variance for depth of penetration.

Source	Sum of Squares	DF	Mean Square	F-value	p-value	
Model	9.80	5	1.96	71.35*	< 0.0001	significant
A-F	1.43	1	1.43	51.97*	< 0.0001	
B-S	4.40	1	4.40	159.97*	< 0.0001	
C-C	1.47	1	1.47	53.52*	< 0.0001	
BC	0.1849	1	0.1849	6.73*	0.0250	
A^2	2.32	1	2.32	84.53*	< 0.0001	
Residual	0.3022	11	0.0275			
Lack of Fit	0.1748	7	0.0250	0.7842	0.6355	not significant
Pure Error	0.1274	4	0.0318			
Cor Total	10.10	16				
$F_{0.05,5,16} = 2.85$	* Significant Variable					

WBW, and ASR were the three types of responses have been taken from each sample (Table 1).

Transverse cross section on each sample has been made in order to measure DOP, WBW, and consequently compute ASR. Next, the cut faces have been smoothly polished and etched to clearly illustrate DOP and WBW using an optical microscope and MIP (microstructural image processing) software. Results of the measuring DOP and WBW have been illustrated in Figure 1.

Modeling and optimization of the process

In this section regression modeling has been used in order to establish the relations between process input variables and output characteristics. Analysis of variance (ANOVA) has also been conducted to statistically analyze and validate the proposed models.[7] Furthermore, percent contribution determination of the input variables on the output characteristics has been performed based on the ANOVA results. When the adequacy of the models has been validated using statistical analysis, a BPNN-based modeling technique has been used in order to model the A-GTAW process and consequently optimize the process in such a way that all the characteristics attain consequently.

Regression modeling and statistical analysis

In order to establish the authentic relations between the process input variables and output characteristics, based on ANOVA results. Table 2, represents the ANOVA results for depth of penetration. The most fitted regression equations for DOP, WBW, and ASP have been proposed (Equations 1–3).

$$
\begin{aligned}
DOP = {}& -21.9 + 0.1187 \times F + 0.425 \\
& \times C - 0.001189 \times (F \times F) - 0.000189 \\
& \times (F \times S) + 0.000435 \times (F \times C) \\
& + 0.000251 \times (S \times S) - 0.000879 \\
& \times (S \times C) - 0.001251 \times (C \times C)
\end{aligned}
\tag{1}
$$

$$
\begin{aligned}
WBW = {}& -97.8 - 0.1743 \times F + 0.4264 \times S \\
& + 1.338 \times C + 0.000561 \times (F \times S) \\
& + 0.000761 \times (F \times C) - 0.001564 \\
& \times (S \times S) + 0.000381 \times (S \times C) \\
& - 0.00630 \times (C \times C)
\end{aligned}
\tag{2}
$$

$$
ASR = e^{-6.60} \times F^{-0.2853} \times S^{2.005} \times C^{-0.392}
\tag{3}
$$

According to ANOVA results, large F–value means that the corresponding process variable makes a big change on the performance characteristic. In this study, a 95% confidence level has been selected to evaluate the variables significances. Therefore, F–values of welding variables have been compared with the appropriate values from confidence table, $F_{\alpha,v1,v2}$; where α is risk, v_1 and v_2 are degrees of freedom associated with numerator and denominator which illustrated in Table 2.[15]

The percent contributions of each A-GTAW process variables on output characteristics have been determined using ANOVA results (Figure 2).[14] For DOP, welding speed acts as the most important variable followed by welding current with 44% and 23% contribution respectively. By the same token, welding speed is the most important variable affects the WBW output characteristics with 30% contribution.

Back propagation neural network modeling

Relating a set of input-output parameters in a system (a manufacturing process such) different procedures are being employed among which artificial neural networks (ANNs) are the most extensively used ones. ANNs are considered as tools capable of relating a set of input and output parameters in different systems. They are reminiscent of the nervous system, which composed of a set of neurons, organized in different layers, and by connections which connect the neurons.[16,17]

The connections between different neurons in different layers are made by means of weighted equations. For each neuron an internal state (activation) proposed, which is a
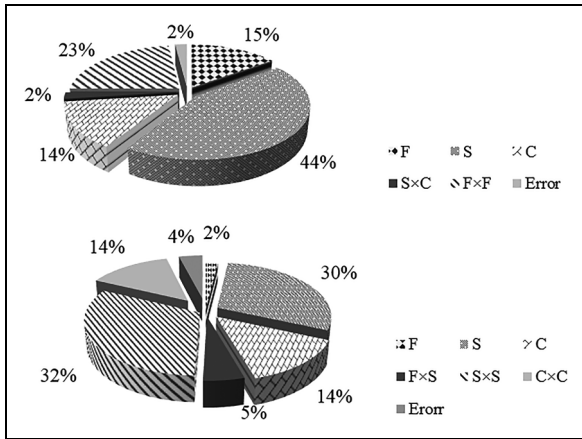
Figure 2. Percent contributions of A-GTAW process variables on DOP and WBW .

function of the input value it is received. Normally, a neuron activation is sent to other neurons as a signal. A weighted activation from other nodes is received by a neuron through its incoming connections. First, a summation function is made by adding these connections. Next, the result is then passed through an activation function, outcome of which being the activation of the node. Then, this activation value is transferred to the next node by multiplication with the specific weight. Weights, bias, and an activation function are the three key components of an ANN. Each neuron receives inputs (x_i, x_j, … x_n) strength of which attached with a weight (w_i). A bias (b_i) can be defined as a type of connection weight with a constant non-zero value added to the summation of weighted inputs ($w_{ij} \times x_j$) forms the input (u_i) to the transfer function. The summation of the input weighted function and bias is given as u_i (Equation (4)).

$$u_i = \sum_{j=1}^{N} w_{ij} x_j + b_i \qquad (4)$$

The most commonly used type of ANNs is feed forward ones equipped with back propagation algorithm known as back propagation neural network (BPNN).[18] In BPNN, an algorithm (back propagation) is employed in which error of each MLP's input-output pair is calculated and then propagated from the last (output) layer to the first (input) layer, adjusting the biases and weights of the MLP network to the error devoted by its neuron proportionally.[18] The details in this regard are well documented in Refs.[16,18]

Commonly, the architecture of BPNN models is determined based on the trial and error. Whereas, in this study in order to eradicate this error, PSO algorithm has been used to determine the proper BPNN's architecture. The hidden layers' number was varied from 1 to 3; hence a **3** (number of process input variables)–n_1–n_2–n_3–**3** (number of process output characteristics) structure was constructed; where the number of neurons/ nodes for the 1st to 3rd hidden layers are n_1, n_2, and n_3 respectively. The training stage acts as a way to find the proper weights and architecture of net that leads to minimum
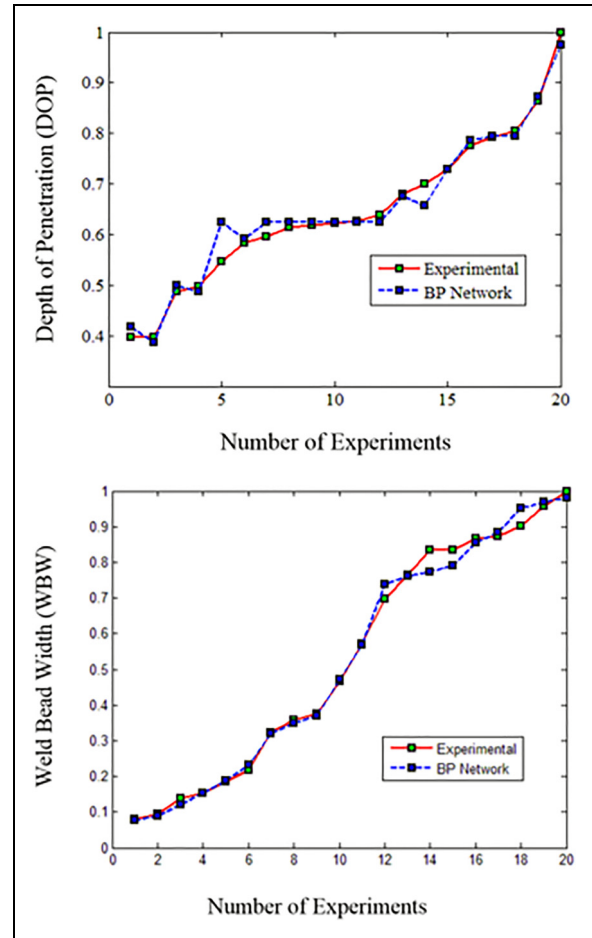

Figure 3. Comparison of process responses and proposed BPNN model predictions.

error between the desired (or predetermined) and predicted measures. The proper proposed BPNN architecture using PSO algorithm was 3-4-4-5-3.

The comparison between process responses and the proposed model predictions has been shown in Figure 3. Figure 4 shows the variation of mean squared error (MSE) during the training process of BPNN model. The performance of the proposed model has been illustrated in Figure 5.

In this study achieving low WBW, high DOP and desired ASR simultaneously required for multi-criteria optimization. Therefore, process multi-responses have been changed into a single measure using Equation (5), where the importance of DOP and WBW have been shown by weighting coefficients of w_1 and w_2 respectively. Based on the literature survey, solidification cracking tendency is significantly influenced by width to depth ratio (WBW to DOP (W/D)), which can be minimized by ensuring that this ratio (ASR) is between 1 and 1.4.[20]

$$\text{Minimize } F\,(F, I, S) = (W_1 \times \text{DOP}) - (W_2 \times \text{WBW}),$$
$$(1.0 < AR < 1.4)\ 25 < F < 75$$
$$100 < I < 120\ 75 < S < 125$$
$$(5)$$

Figure 4. Variation of mean squared error (MSE).
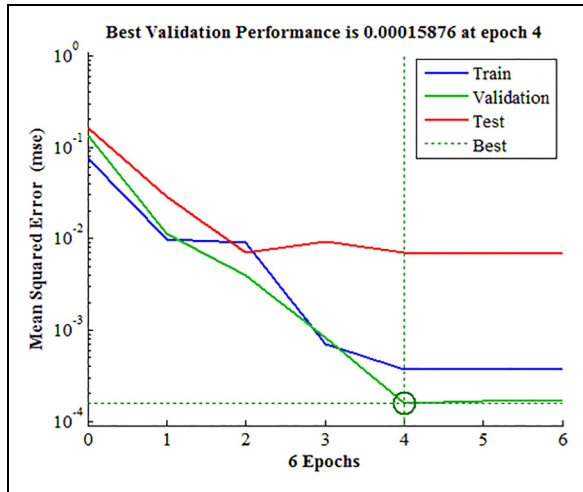

Figure 5. Performance of the proposed BPNN model in training, validation and test stages.

Simulated annealing algorithm

As different algorithms (including simulated annealing (SA), genetic (GA), Tabu search (TS), ant colony (AC), bee colony (BC), particle swarm optimization (PSO), and etc.,) have different procedures for finding the optimum condition, they are used for different optimization purposes. Among the proposed algorithms PSO and SA, due to their advantages are mostly being employed. Easy programming (few input parameters to adjust) and fast convergence are the major merits of PSO algorithm. Whereas, in high dimensional space, falling into local optimum traps may be considered as a weakness for PSO algorithm. Based on the SA mechanism this algorithm could avoid getting trapped into local optimum which can be considered as a major excellence over other algorithms.[20]

In this study, PSO and SA algorithms due to their mentioned merits, have been employed as the heuristic algorithms to optimize A-GTAW process variables in order to achieve maximum DOP, minimum WBW and proper value of ASR simultaneously. In this study, PSO has been used twice (to determine the most appropriate architecture for BPNN model and optimize the process variables). Next, SA algorithm has been used to evaluate the performance of PSO algorithm. Furthermore, a set of validation experiments has been conducted in order to confirm the proposed approach.

All heuristic algorithms are reminiscent of biological or physical processes. In this regard, SA algorithm is reminiscent of annealing in heat treatment process.[21,22] In annealing process, metals are heated up to a specific and pre-determined temperature (near the melting point), at which all metal particles are in random motion. Then, all metal particles rearranged by cooling down slowly toward the lowest energy state. As the cooling process is conducted appropriately slowly, lower and lower energy states are achieved until the lowest energy state is reached. Similarly, in A-GTAW process the 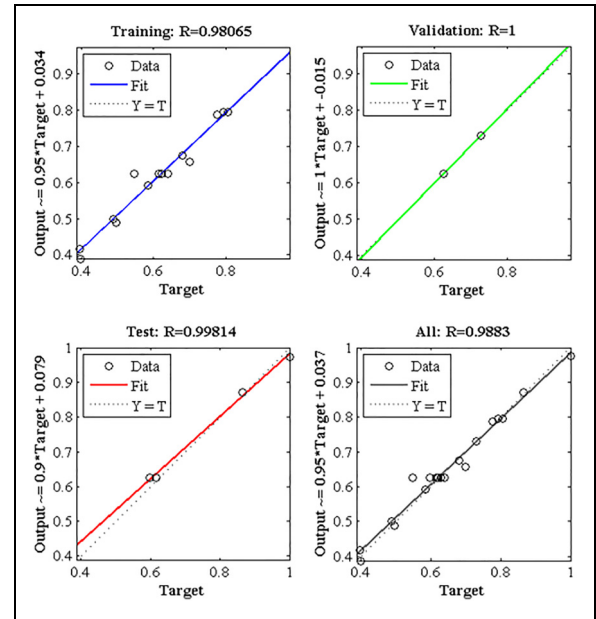lowest energy level gives the optimized value for variables based on an energy function is created and minimized. The mechanism of SA algorithm is defined as follows[23]:

Defining an acceptable answer space and generating an initial random solution in this space. Next, the new solution's objective function (C_1) is computed and compared with the current ones (C_0). A move to a new solution is made either the new solution has better value or the value of SA probability function (Equation (6)) is higher than a randomly generated number between 0 and 1[22]:

$$P_r = \exp\left(-\frac{\Delta C}{T_k}\right) \tag{6}$$

Where, temperature parameter is shown by T_k, which acts as the temperature in the physical annealing process does.[21] Equation (7), is used as a temperature reduction rate to cool down the pre-determined temperature at each iteration.[22]

$$T_{k+1} = \alpha \times T_k \quad k = 0, 1, \ldots \text{ and}$$
$$0.9 \le \alpha < 1 \tag{7}$$

Where, the current and former temperatures are shown by T_{k+1} and T_k respectively. The cooling rate also presented by parameter α. Consequently, at the first iterations of SA due to higher temperature, most of the not improving (or even worsening) moves may be accepted. Nonetheless, as the algorithm proceeds and temperature is reduced only improving moves are likely to be accepted. This strategy could help the algorithm avoid being trapped in local minimum and jump out of it. After a specific number of iterations, a number of iterations in which no development is detected, and a pre-determined run time, the algorithm may be dismissed.
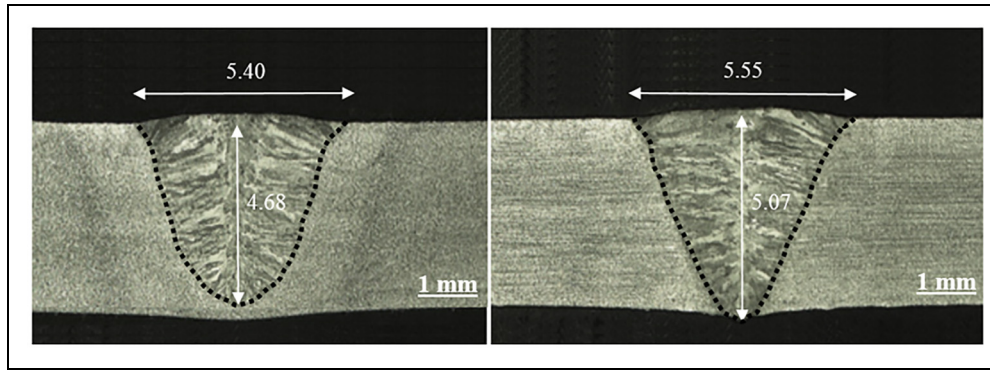
Figure 6. Evaluation of DOP and WBW for the optimized condition based on SA and PSO algorithms.
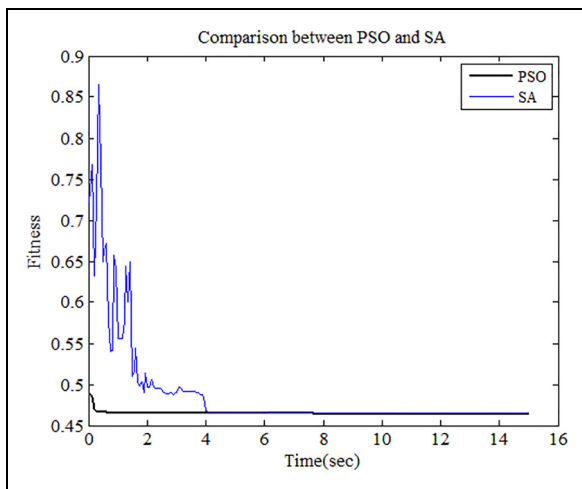

Figure 7. Convergence of heuristic (PSO and SA) algorithms.

Particle swarm optimization algorithm

PSO is a heuristic algorithm proposed by Kennedy and Eberhart.[24] It begins with a population of random solutions which is updated and searched for optimum ones. The current optimum particles are followed by the random solutions (known as particles) through the problem space. The problem space is connected with the best obtained solution and its corresponding location shown by "pBest" and "gBest" respectively. Each particle keeps track of the "pBest" and "gBest" in the problem space by changing its velocity towards them. The following Equations (8 and 9) used updating the particles.[25–27]

$$V_{i+1} = w \times V_i + (C_1 \times r_i \times (pBest_i - X_i)) + (C_2$$
$$\times r_i \times (gBest_i - X_i)) \tag{8}$$

$$X_{i+1} = X_i + V_{i+1} \tag{9}$$

Where, (V_{i+1}) for each particle has been determined based on its previous velocity (V_i), global best solution (pBest) and location (gBest). Equation (9) has been used for updating the particle's position (X_i).[27] The terms "r_1" and "r_2" are two random numbers generated independently in the range of [0, 1]. There are acceleration

constants ("c_1" and "c_2") using which pull each particle (solution) towards "pBest" and "gBest" positions. Inertia weight "w", acts as an important parameter in PSO algorithm convergence behavior. In order to explore the answer space globally, the large amount of "w" required, while the small amounts explore nearby regions of the space.[28]

Based on the literature survey, the architecture (number of hidden layers and nods in hidden layers) of BPNN in most studies has been determined using trial and error. Whereas, in this study PSO algorithm has been employed to determine the PBNN architecture. Furthermore, the optimization of the proposed BPNN models have been carried out using PSO algorithm. Moreover, SA algorithm has been used to confirm the performance of PSO algorithm (avoiding getting trapped in the local optima).

The performance of each evolutionary algorithm is affected by its own distinctive adjusting parameters. The details of the PSO performance are well documented in Refs.[24–27]

The adjusting parameters used for controlling the SA and PSO algorithms are carried out as the following:

- *PSO variables:* Population: 50; Learning factor c_1 and c_2: 2; Number of iteration performed: 30.
- *SA variables:* Temperature reduction rate: 0.91; Processing time: 30; seconds Initial temperature: 700.

Apart from using the proposed method for modeling and optimization purposes (hybrid BPNN-PSO, BPNN-SA), the design expert software (version 11) provides an optimization technique for optimization of BBD.

Results and discussion

In this study first, BBD based on RSM has been employed to determine the experimental design matrix required for data gathering, modeling and optimization purposes. Next, DOP and WBW values have been measured using MIP software. Based on the results of WBW and DOP, ASR values have been computed. Then, regression modeling has been used to establish the relations between

Table 3. Optimal A-GTAW process variables and coressponding process measures.

Output	Algorithm	Process variables F	S	C	Predicted	Experimental	Error (%)
$W_{DOP} = 0.50$ and $W_{WBW} = 0.50$							
DOP	PSO	74	133	100	4.96	5.07	2.2
WBW	PSO	74	133	100	5.63	5.55	2.4
ASR	PSO	75	134	100	1.13	1.10	3.0
DOP	SA	75	134	100	4.81	4.68	2.7
WBW	SA	75	134	100	5.62	5.40	3.9
ASR	SA	74	133	100	1.17	1.15	2.0
DOP	BBD	64	131	103	5.00	4.82	3.6
WBW	BBD	64	131	103	6.00	6.20	3.3
ASR	BBD	64	131	103	1.22	1.28	3.1

process input (welding speed, current and percentage of activating fluxes combination) and output (DOP, WBW and AR) parameters. ANOVA has been employed to statistically analysis the adequacy of the proposed models and determine the percent contribution of process variables on the output characteristics. BPNN has been employed to model the A-GTAW process. Moreover, in order to determine the proper BPNN architecture, PSO algorithm has been used. Then, PSO algorithm has been used again to optimize the proposed proper BPNN model in such a way that DOP increased and WBW decreased and achieved the desired ASR simultaneously. Furthermore, the PSO algorithm performance has been checked using SA algorithm. Moreover, based on the importance given to DOP and WBW in A-GTAW process, different weights (W_1 and W_2) could have been considered (Equation (5)). In this study the value of 0.5 has been considered for W_1 and W_2. Figure 6, illustrates the cross section of weldments which have been optimized using BPNN-SA and BPNN-PSO procedures. The convergence of PSO and SA algorithms have been shown by Figure 7. Based on the nature of the PSO algorithm, its convergence is faster than SA algorithm. Table 3, represents the results of BPNN-PSO, BPNN-SA, and BBD optimizations. Based on the results, PSO and SA algorithms could accurately optimize the process responses (maximum 4% error). Comparing the results with the latest published research using RSM for optimization purposes is found to be an accurate technique for modeling and optimizing the A-GTAW process variables in order to obtain the maximum DOP, minimum WBW and desired ASR in AISI316Lstainless steel alloy. In this regard, the second-order quadratic model has been successfully used to predict the DOP during A-GTAW process of duplex stainless steel plates.[28] Based on the ANOVA results, the current has more percentage contribution on DOP (83.88%) followed by torch speed (8.33%). Setting the A-GTAW process variables at 200 A welding current, 1 mm electrode gap, 10 lit/min gas flow rate, 100 mm/min welding speed ended in the optimum condition using Taguchi technique.[29] Moreover, the percentage contribution of process

variables for tensile strength have been investigated as welding speed (45%), welding current (28%), arc gap (21%) and gas flow rate (6%).[30] Considering these studies revealed that the effect of percentage of activating fluxes combination and modeling of the process have been neglected. Moreover, the optimization process has been conducted based on only one method (e.g. Taguchi technique, RSM, and etc.). In this study, the modeling procedure has been carried out using regression and artificial neural network method. Furthermore, the optimization process has been conducted and compared using three methods (BPNN-PSO, BPNN-SA, and BBD).

Conclusion

Apart from different merits have been considered for GTAW process, poor penetration is the most important demerit of this process. To cope with the mentioned shallow penetration different procedures have been proposed among which A-GTAW process is the most important and extensively used one which has been considered in this study to be modeled and optimized. The modeling and optimization of A-GTAW process for AISI316L austenite stainless steel parts considering both the process input variables and percentage of activating fluxes combination has been addressed throughout this study. Based on the ANOVA results all the welding variables (welding speed, welding current and percentage of activating fluxes combination) have been significant (using F–test and $F_{\alpha, v1, v2}$ value) among which welding speed was the most important variable affecting the both DOP and WBW with 44% and 30% contribution respectively. In this study three method of optimization have been proposed (BPNN-PSO, BPNN-SA, and BBD). Although, the three optimization methods have been converged to the same results, the BPNN-PSO had the best performance with average 2.5% error followed by BPNN-SA and BDD with average error of 2.8% and 3.33% errors respectively. Using the proposed hybrid BPNN-PSO approach either process input variables have been optimized (133 mm/sec for welding speed and 100 Amp for welding current) and the optimum formula (74% SiO_2

and 26% TiO$_2$) for activating fluxes combination has been determined in order to achieve the desired process output measures. Moreover, maximum DOP (5.07 mm), minimum WBW (5.55 mm) and desired ASR (1.1 mm) have been achieved simultaneously using BPNN-PSO procedure. The result of proposed optimization procedure showed that the proposed method can precisely simulate and optimize (with less than 4% error) the A-GTAW process.

Declaration of conflicting interests

The author(s) declared no potential conflicts of interest with respect to the research, authorship, and/or publication of this article.

Funding

ORCID iD

Farhad Kolahan https://orcid.org/0000-0002-7119-6704

References

1. Sivakumar J, Vasudevan M and Korra N. Effect of activated flux tungsten inert gas (A-TIG) welding on the mechanical properties and the metallurgical and corrosion assessment of inconel 625. *Weld World* 2021; 65: 1061–1077.
2. Neelima P, Agilan M, Saravanan K, et al. Optimisation of flux and weld parameters during flux bounded tungsten inert Gas welding (FBTIG) of nickel based superalloy inconel 600. *Trans Indian Nat Acad Eng* 2021; 6: 123–131.
3. Sivakumar J and Korra NN. Optimization of welding process parameters for activated tungsten inert welding of inconel 625 using the technique for order preference by similarity to ideal solution methodology. *Arab J Sci Eng* 2021; 46: 7409–7418.
4. Dhananjay S, Bhagwan S, Shrikant F, et al. Effect of different activated fluxes on mechanical properties of DSS 2205 in pulsed tungsten inert Gas welding. *Adv Additive Manuf Joining* 2021; 54: 619–629.
5. Vidyarthy RS and Dwivedi DK. Microstructural and mechanical properties assessment of the P91 A-TIG weld joints. *J Manuf Process* 2018; 31: 523–535.
6. Lippold JC and Kotecki DJ. *Welding metallurgy and weldability of stainless steels*. WILEY, 2005.
7. Pamnani R, Vasudevan M, Vasantharaja P, et al. Optimization of A-GTAW welding parameters for naval steel (DMR 249 A) by design of experiments approach. *J Mater Design Appl* 2015; 34: 1–12.
8. Arivazhagan B and Vasudevan M. Studies on A-TIG welding of 2.25 Cr–1Mo (P22) steel. *Mater Manuf Processes* 2015; 18: 55–59.
9. Arivazhagan B and Vasudevan M. A comparative study on the effect of GTAW processes on the microstructure and mechanical properties of P91 steel weld joints. *Mater Manuf Processes* 2014; 16: 305–311.
10. Kurtulmus M. Effects of welding parameters on penetration depth in mild steel A-TIG welding. *Scientia Iranica B* 2019; 26: 1400–1404.
11. Kumar VB, Lucas D, Howse G, et al. Investigation of the A-TIG Mechanism and the Productivity Benefits in TIG Welding. Fifteenth International Conference on the Joining of Materials, 15 December 2009.
12. Venkatesan G, George J, Sowmyasri M, et al. Effect of ternary fluxes on depth of penetration in A-TIG welding of AISI 409 ferritic stainless steel. *Proc Mater Sci* 2014; 5: 2402–2410.
13. Chern TS, Tseng KH and Tsai HL. Study of the characteristics of duplex stainless steel activated tungsten inert gas welds. *Mater Des* 2011; 32: 255–263.
14. Tathgir S and Bhattacharya A. Activated-TIG welding of different steels: influence of various flux and shielding gas. *Mater Manuf Processes* 2015; 31: 335–342.
15. Martínez VM, Gomez-Gil FJ, Gomez-Gil J, et al. An artificial neural network based expert system fitted with genetic algorithms for detecting the status of several rotary components in agro-industrial machines using a single vibration signal. *Expert Syst Appl* 2015; 42: 6433–6441.
16. Markopoulos AP, Manolakos DE and Vaxevanidis NM. Artificial neural network models for the prediction of surface roughness in electrical discharge machining. *J Intell Manuf* 2008; 12: 283–292.
17. Sahin H and Topal B. Impact of information technology on business performance: integrated structural equation modelling and artificial neural network approach. *Scientia Iranica B* 2018; 25: 1272–1280.
18. Kurtulmus M and Kiraz A. Artificial neural network modelling for polyethylene FSSW parameters. *Scientia Iranica B* 2018; 25: 1266–1271.
19. Kou S. *Welding metallurgy*. Hoboken, New Jersey, New Jersey, USA: John Wiley & Sons, 2003/9.
20. Magudeeswaran G, Sreehari R, Sundarb L and Harikannana N. Optimization of process parameters of the activated tungsten inert gas welding for aspect ratio of UNS S32205 duplex stainless steel welds. *Defense Technology* 2014; 10: 251–260
21. Beheshti Z, Mariyam S and Shamsuddin H. A review of population-based meta-heuristic algorithm. *Int J Adv Soft Comput* 2013; 5: 1–36.
22. Jahromi MHMA, Tavakkoli Moghaddam R, Makui A, et al. Solving a one-dimensional cutting stock problem by simulated annealing and tabu search. *J Indust Eng Int* 2012; 8: 1–8.
23. Ayubi Rad MA and Ayubi Rad MS. Comparison of artificial neural network and coupled simulated annealing based least square support vector regression models for prediction of compressive strength of high-performance concrete. *Scientia Iranica A* 2017; 24: 487–496.
24. Lee KH and Kim KW. Performance comparison of particle swarm optimization and genetic algorithm for inverse surface radiation problem. *Int J Heat Mass Transfer* 2015; 88: 330–337.
25. Zhi K, Jia W, Zhang G, et al. Normal parameter reduction in soft set based particle swarm optimization algorithm. *Appl Math Model* 2015; 39: 4808–4820.
26. Azadi Moghaddam M and Kolahan F. Modeling and optimization of the electrical discharge machining process based on a combined artificial neural network and particle swarm optimization algorithm. *Scientia Iranica B* 2020; 27: 1206–1217.
27. Hasheminejad MM, Sohankar N and Hajiannia A. Predicting the collapsibility potential of unsaturated soils using adaptive

neural fuzzy inference system and particle swarm optimization. *Scientia Iranica A* 2018; 25: 2980–2996.

28. Azadi Moghaddam M, Golmezergi R and Kolahan F. Multi-variable measurements and optimization of GMAW parameters for API-X42 steel alloy using a hybrid BPNN–PSO approach. *Measurement* 2016; 92: 279–287.

29. Korra NN, Vasudevan M and Balasubramanian KR. Optimization of A-TIG welding of duplex stainless steel alloy 2205 based on response surface methodology and experimental validation. *Proc IMechE Part L: J Materials: Design and Applications* 2018; 12: 1–10.

30. Lugade PS and Deshmukh MJ. Optimization of process parameters of activated tungsten inert Gas (A-TIG) welding for stainless steel 304L using taguchi method. *Int J Eng Res Gen Sci* 2015; 3: 2091–2730.